GEOMETRY OF NORMAL MAMMALIAN PLATELETS BY QUANTITATIVE MICROSCOPIC STUDIES

M. M. FROJMOVIC *and* R. PANJWANI

From the Department of Physiology, McGill University, Montreal, Quebec H3C 3G1, Canada

ABSTRACT The shape distributions of normal and hardened human and rabbit erythrocytes and platelets were obtained for edge-on orientations of a few hundred freely rotating cells from analyses of microphotographs obtained similarly as by Ponder (1930, *Q. J. Exp. Physiol.* **20**:29) by phase-contrast microscopy at 800× magnification. Major average diameters ($\bar{d}$) and thicknesses ($\bar{t}$) were estimated for both normal and hardened cells, and were used to calculate an average geometric axis ratio, $\bar{r}_p = \overline{t/d}$, which increases to unity as cells become more spherical. Our fixation procedure did not alter these shape parameters: $\bar{r}_p$ was unchanged for erythrocytes, with $\bar{d}$ and $\bar{t}$ values similar to those reported by Ponder (1930); platelets had $\bar{d} \times \bar{t} = 3.6 \pm 0.7\ \mu m \times 0.9 \pm 0.3\ \mu m$ and $3.1 \pm 0.4\ \mu m \times 0.6 \pm 0.3\ \mu m$, respectively, for human and rabbit cells, with $\bar{r}_p = 0.26$ and 0.20, respectively. Agreement in $\bar{r}_p$ was found with data obtained by a novel rheo-optical method which allows for a direct statistical averaging for large populations ($>100 \times 10^3$ cells). Histograms and linear correlation studies were made of the above three parameters (d, t, r_p), as well as volume (V), total surface area (S), and sphericity index (S. I.) calculated for both "prolate ellipsoid" and "disc with rounded edges" models. Results indicate very high linear correlations between $r_p - t$, $r_p -$ S. I., and $d - S$, with high correlations for $t - V$, $d - V$ and $V - S$. Data are in agreement with the few reports in the literature determined by other methods, with the best model for platelets appearing to be an oblate spheroid.

INTRODUCTION

Accurate information on the geometry of erythrocytes and platelets is of interest in order to study the mechanics of cell deformation and microrheology in the microcirculation (Evans and Fung, 1972; Frojmovic et al., 1975; Goldsmith and Marlow, 1972); to study the relationships between cell geometry and function with changes in cell environment, cell age, and health and age of the human donors themselves; and to provide quantitative geometric data to allow theoretical calculations for statistical methods using light transmission in stirred suspensions (Frojmovic and Panjwani, 1975) or in sheared suspension (rheo-optics) for assessing cell geometry and geometric changes from measurements of mean hydrodynamic axis ratios (Frojmovic, 1975; Frojmovic et al., 1975; 1976). Some studies have been made on the change in size of human erythrocytes (Child et al., 1970) and of platelets (Bigel et al., 1967*a*,*b*; Entick-

nap et al., 1969; Garg et al., 1971; Kraytman, 1973) with known disease states using light microscopy. Such studies relating cell shape, rather than size, have only been made with electron microscopy (Bessis, 1973; Lechner et al., 1969).

Size and shape studies of erythrocytes were begun by Ponder (1930) by direct light microscopy studies on native cells, observed both face-on and edge-on, with empirical evaluations of the cell outlines. This approach has been continued in terms of correlation studies between erythrocyte thickness (t), diameter (d), surface area (S), volume (V), and a shape factor called the sphericity index (S. I.), with both brightfield (Canham and Burton, 1968; Jay, 1975) and interference-holographic microscopy (Eden, 1972; Evans and Fung, 1972; Evans and Leblond, 1973; Tsang, 1974). Such studies have not been reported to date for blood platelets, which have been generally qualitatively analyzed for size and shape with phase-contrast microscopy (Bessis, 1973; Bigel et al., 1967*a*,*b*; Garg et al., 1971; Zucker and Borrelli, 1954) and with electron microscopy (Barnhart et al., 1972; Hovig, 1968; Lechner et al., 1969; Shimamoto et al., 1973). These studies of individual platelets have been almost exclusively limited to platelets settled or spread onto supporting surfaces (Bessis, 1973). We thus present, for the first time, geometric data from light microscopy studies of human and rabbit platelets freely rotating in suspension.

MATERIALS AND METHODS

Cell Suspensions

Human and rabbit blood was drawn by venipuncture and ear arterial puncture, respectively, into 3.8% citrate (1 vol to 9 vol of blood), centrifuged at 100*g* and 180*g*, respectively, at 37°C, to obtain platelet-rich plasma (PRP) which was removed. The top 5% of the erythrocyte layer was discarded and the remainder of the loosely packed erythrocyte suspension as well as the PRP were appropriately diluted with plasma (37°C) or were fixed with a solution of 0.6% glutaraldehyde in Tyrode's solution (50% glutaraldehyde solution diluted with Tyrode at pH = 7.4) at 37°C, 1 vol of suspension to 3 vol of aldehyde, thereafter incubating for $\frac{1}{2}$ h at 37°C. Fixation was effected within 1 h of the PRP preparation, with apyrase added to citrated blood (1.0 mg/ml blood) in one of the human cell preparations. These suspensions were then directly analyzed as described below after appropriate dilution of hardened erythrocytes with Tyrode's solution at pH = 7.4, no further dilution being necessary for the hardened platelet suspension.

Phase Contrast Microphotography

A small drop of cell suspension was transferred to the center of a 20 mm × 20 mm area in the middle of a glass slide surrounded by a very thin layer of Vaseline. A clean 22 mm × 22 mm no. 1 coverslip was placed gently over this rectangular space so as to avoid air bubbles. Slight pressure was applied over the cover glass to spread the sample evenly, with the Vaseline forming a seal around it.

Photography was done through a Carl Zeiss Ultra Phot. II microscope (Carl Zeiss, Inc., New York), using phase contrast with a nominal magnification of 800× (40 × objective), and a green filter, with a camera shutter speed of $\frac{1}{4}$ s and TRI-X (400 ASA) black and white film. A tungsten lamp was used in all cases. Calibration was made with a stage micrometer

(Olympus, Tokyo). A few photographs were also taken using the interference Nomarski optics, with flash photography and 80 ASA film.

Each negative in the processed film was magnified about 1,000× using a slide projector and screen, and cell measurements were made with a transparent plastic ruler, accurate to within ±0.1 mm = ±0.1 μm. Cell sizes and outlines are typically depicted in Fig. 1.

The longer and shorter axes of the ellipsoidal platelets in side view were designated as d (diameter) and t (thickness), respectively (Fig. 1), while comparable diameters (d') were obtained from face-on views (Fig. 2). Unless otherwise specified, our d and t values for blood cells are reported for d_{av} and t_i dimensions from edge-on views of cells (Fig. 1), as originally recommended by Ponder (1930). Dozens of pictures were taken for any one preparation as only cells in the plane of focus were analyzed, as determined by the following two criteria: (*1*) the dark diffraction ring observed for edge-on views of both erythrocytes and platelets was always asymmetrical when the platelets rotated away from the edge-on position, and (*2*) it became diffuse when the cell was out of focus. Note that the projected d_{max} should be unaffected by particle rotation about the minor axis.

Bias in the Samples: Platelet-rich Plasma vs. Whole Blood

The studies of platelet dimensions are here reported for platelet-rich plasma, which is a supernatant suspension remaining after gentle packing of erythrocytes and leukocytes (Frojmovic and Panjwani, 1975), and which may therefore not contain the larger platelets that may have sedimented to the top of the red cells or within, as reported by Nakeff and Ingram (1970) for different PRP preparations. We therefore estimated the percentage of large cells in citrated whole blood diluted 100-fold with 1% ammonium oxalate solution (yielding lysed erythrocytes and "sphered" platelets), as compared with those in glutaraldehyde-treated PRP, using Wright's stain to distinguish leukocytes, and counting a volume of 0.9 μl in the hemocytometer. The platelet yield for PRP (%) was determined from the volumes of whole blood (V_B) and PRP (V_p), and associated platelet counts (N_B and N_p expressed as number per microliter):

$$\text{Platelet yield (\%)} = (V_p \cdot N_p / V_B \cdot N_B) \cdot 100. \quad (1)$$

Finally, note that "sphered" platelets (Fig. 2C), readily distinguishable from discs (Fig. 2B) and representing about 5–10% of all cells present in citrated PRP, were not measured.

Calculations

The two cellular dimensions obtained from edge-on observations of platelets (d, t) were entered into a PDP-15 computer. Fortran-programs were written to determine the four parameters as defined below, with their corresponding histograms and associated shape represented by the standard statistical parameters[1]: moments, skewness, and kurtosis, as well as linear correlation coefficients obtained between these parameters. The programs also allowed plotting of the histograms, as well as data points with the theoretical line shown based on an analysis of linear regression.

The generated parameters were:

$$\text{Geometric axis ratio, } r_p = t/d. \quad (2)$$

---

[1] Rth moment $\pi_R = (X_i - \bar{X})^R/N$ (N = number of entries); skewness = $\pi_3/\pi_2^{3/2}$ (0 for symmetrical curve, ± for skewed); kurtosis = π_4/π_2^2 (Gaussian dist^n = 3.0; for platykurtic dist^n [flat topped] < 3.0; for leptokurtic dist^n [peaked] > 3.0). Skewness indicates a preponderance of measurements on one side of the mean, while kurtosis indicates the degree of peakedness in the distribution curve due to the shift of central and extreme values towards or away ±1 SD from the mean.

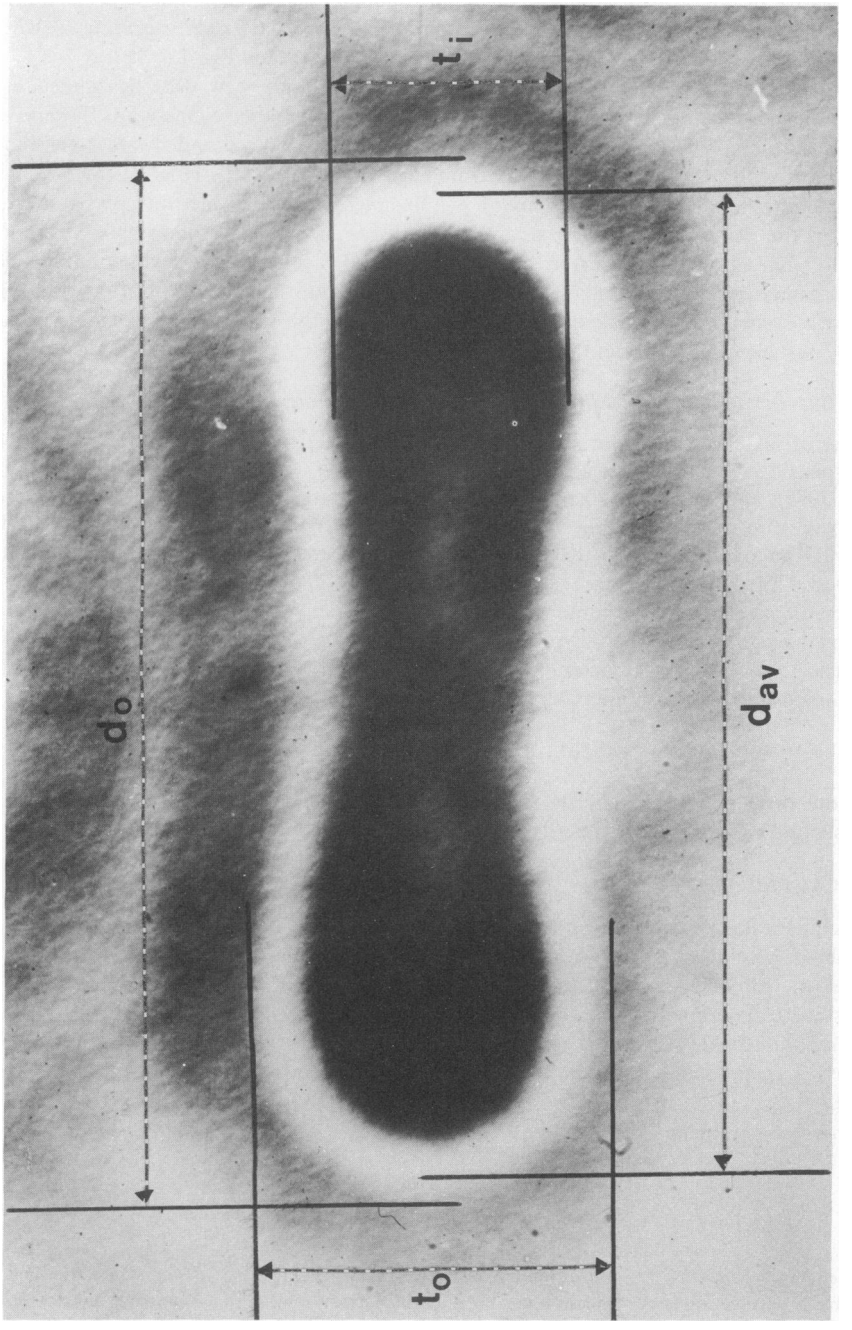

FIGURE 1A

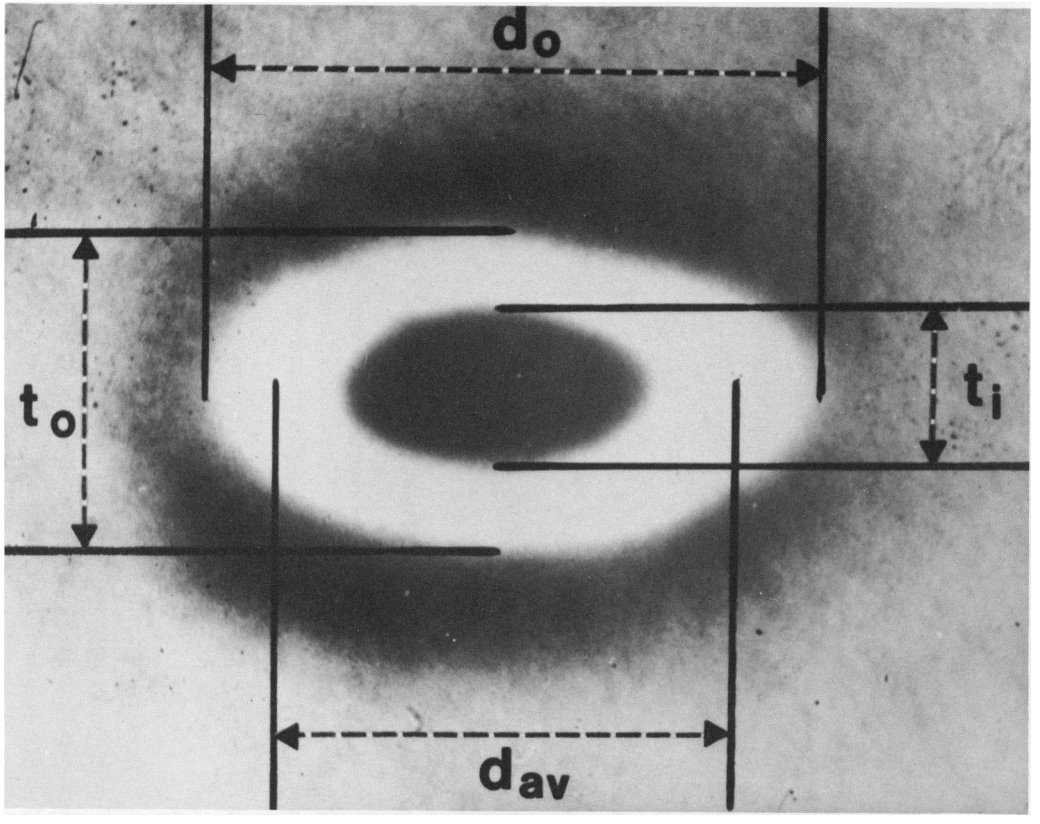

FIGURE 1B

FIGURE 1 Profiles of erythrocytes (*A*) and platelets (*B*) as viewed on edge for measurement of maximum diameter and thickness. Positive print, as observed in the microscope objective with phase-contrast, at 800 × magnification. We have delineated inside (d_i) and average values (d_{av}; midway between inside and outside diffraction rings). Edge-on views present a white center; face-on views (Fig. 2B) present a dark center; while "sphered" cells (Fig. 2C) are homogeneously white and readily distinguishable.

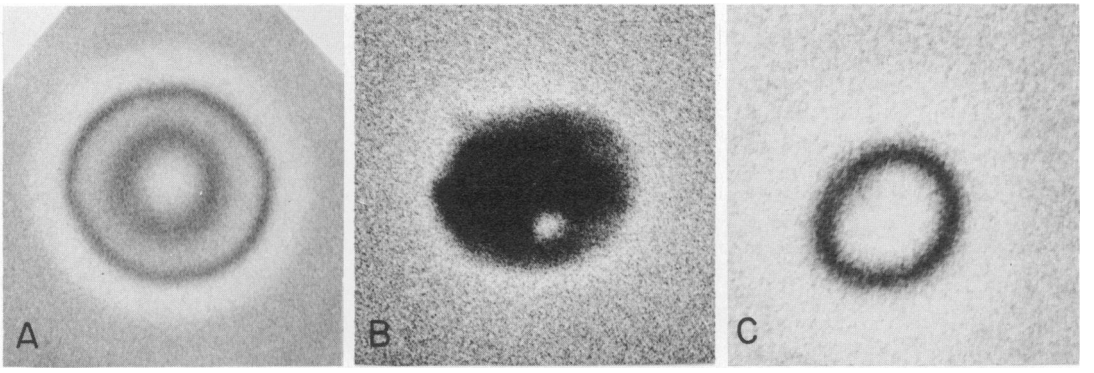

FIGURE 2 Photomicrographs by phase-contrast microscopy as in Fig. 1, of face-on views of erythrocytes (*A*); and platelets, for a normal disc (*B*) and ADP-sphered particle (*C*).

For the platelet represented by an oblate spheroid (Weast, 1968):

$$\text{Volume, } V = (\pi/6) \cdot d^2 t, \tag{3}$$

$$\text{Surface area, } S = (\pi/2) \cdot d^2 + (\pi/4) \cdot t^2[(1 + r_p)/(1 - r_p)] \log r_p^{-1}. \tag{4}$$

For the "disc with rounded edges" model:

$$\text{Volume, } V = (\pi/4)d^2 t + (\pi/6)t^3 + (\pi^2/8)dt^2, \tag{5}$$

$$\text{Surface area, } S = (\pi/2)(d^2 + t^2) - (\pi^2/4)t^2, \tag{6}$$

$$\text{Sphericity index (Rand and Burton, 1963), S. I.} = 4.84 \cdot V^{2/3}/S. \tag{7}$$

Note that r_p and S. I. are both dimensionless constants with values ranging from zero for a laminar disc to unity for a sphere. The latter has been used exclusively in the study of erythrocyte geometry in recent years and is therefore included in our present studies.

THE SIZE AND SHAPE OF MAMMALIAN PLATELETS

Results

As seen in Fig. 1 there are unavoidable diffraction rings associated with the photomicrographs of edge-on orientations of erythrocytes and platelets arising from the interaction of light whose wavelength approaches the actual thickness of the particle being analyzed, as first reported by Ponder (1930) for erythrocytes. There is still no theoretical basis, however, for choosing the true geometric outlines in these photomicrographs. Evans and Fung (1972) have estimated that the red cell thickness derived from such photographs would be subjected to an uncertainty of the order of 20%. We have therefore separately measured $\bar{d}_{av}$ and $\bar{t}_i$, as well as $\bar{d}_o$ and $\bar{t}_o$ (as shown in Fig. 1), and calculated mean values (±SD) with corresponding mean axis ratios ($\bar{r}_p$), for both normal and glutaraldehyde-hardened rabbit erythrocytes, as well as for a few normal human erythrocytes. These results are shown in Table I-A, where the $\bar{d}_{av}$, $\bar{t}_i$, and $\bar{r}_p$

TABLE I

GEOMETRY OF NORMAL AND HARDENED ERYTHROCYTES AND PLATELETS FROM HUMANS AND RABBITS

Cell type	No. of donors	Diameter* $\bar{d} \pm$ SD	Thickness* $\bar{t} \pm$ SD	Geometric axis ratio† $\bar{r}_p \pm$ SD	No. of cells	Comment
		μm	μm			
A. Erythrocyte						
Rabbit						
Normal	2	7.3 ± 0.4	2.2 ± 0.2	0.30 ± 0.05	36	
		$(7.3 \pm 0.4$	1.7 ± 0.1	$0.24 \pm 0.02)$		Ponder (1930)
		$[7.9 \pm 0.4$	3.3 ± 0.2	$0.42 \pm 0.05]$	36	d_o, t_o
Hardened	2	7.3 ± 0.4	2.1 ± 0.2	0.29 ± 0.04	23	
		$[7.7 \pm 0.4$	3.0 ± 0.2	$0.39 \pm 0.05]$	23	d_o, t_o
Human						
Normal	1	8.50 ± 0.30§	2.50 ± 0.20	0.29 ± 0.04	50	
	5	$(8.55 \pm 0.40$	2.40 ± 0.10	$0.28 \pm 0.03)$	500	Ponder (1930)
		$[9.1 \pm 0.4$	3.5 ± 0.3	$0.39 \pm 0.05]$	50	d_o, t_o
	1	7.82 ± 0.62	2.58 ± 0.27	0.34 ± 0.06	50	Evans (1972)‖
B. Platelet						
Rabbit						
Normal	3	3.00 ± 0.40	0.63 ± 0.30	0.20 ± 0.10	65	
Hardened	4	3.10 ± 0.43	0.62 ± 0.19	0.21 ± 0.07	158	
		$[3.90 \pm 0.70$	1.50 ± 0.20	$0.39 \pm 0.10]$	65	d_o, t_o
Human						
Hardened	2¶	3.64 ± 0.72**	0.92 ± 0.34	0.26 ± 0.09	46	
	4	$(3.75 \pm 0.47$	0.96 ± 0.09	$0.26 \pm 0.06)$	TEM††	
		$[4.0 \pm 0.7$	2.0 ± 0.3	$0.50 \pm 0.15]$	46	d_o, t_o

*$\bar{d}_{av}$ and $\bar{t}_i$ are normally reported, but corresponding values for d_o and t_o are shown in square brackets (see Fig. 1).

†$\bar{r}_p = \bar{t}/\bar{d}$ for erythrocytes; $\bar{r}_p = \bar{t}/\bar{d} = \overline{t/d}$ ($\pm$ 3%) for platelets.

§Face-on measurements of $\bar{d}$ for normal and fixed human cells: $8.3 \pm 0.4\ \mu m$ ($n = 15$) and $8.5 \pm 0.4\ \mu m$ ($n = 7$), respectively.

‖ Interference holographic method: Tsang (1974) found similar results for 1,500 cells analyzed.

¶Combined values of two male subjects = one 18 yr old ($n = 10$) ≡ one 40 yr old ($n = 36$).

**Face-on measurements (see Fig. 2) for hardened platelets gave $\bar{d}_i = 4.1 \pm 0.6\ \mu m$ and $\bar{d}_{av} = 4.5 \pm 0.6\ \mu m$ ($n = 31$).

††Lechner et al. (1969). d_{max} and t_{max} measured from 0.5 μm sections in transmission electron microscopy (TEM).

values compare well with results reported by others. No significant geometric changes (t, d) occurred on fixation of rabbit or human erythrocytes, as described in the experimental section (Table I-A). This was indeed equally true for comparisons of mean diameters determined for face-on views of both normal and hardened erythrocytes (Fig. 2A), with $\bar{d}_i = 7.1 \pm 0.4\ \mu m$ ($n = 20$) and $\bar{d}_{av} = 8.8 \pm 1.0\ \mu m$ ($n = 18$) for rabbit erythrocytes, and $\bar{d}_{av} = 8.4 \pm 0.5\ \mu m$ ($n = 15$) for human erythrocytes. We must note that $\bar{d}_{av}$ edge-on = $\bar{d}_{av}$ face-on for human erythrocytes, while for the smaller rabbit erythrocytes, it was less than $\bar{d}_{av}$ face-on but equal to $\bar{d}_i$ face-on.

A smaller description is given in Table I-B, for both normal and hardened rabbit platelets and hardened male human platelets, with $\bar{d}_{av}$ and $\bar{t}_i$ found almost identical to

values reported from analyses of transmission electron micrographs (Table I-B). Fixation did not significantly alter rabbit platelet geometry as found for erythrocytes, while the same was assumed for human platelets. Finally, we should note that as observed for rabbit erythrocytes, face-on measurements of human hardened platelet diameters gave $\bar{d}_i = 4.1 \pm 0.6\ \mu m$, only 10% larger than $\bar{d}_{av}$ estimated from edge-on measurements, while $\bar{d}_{av} = 4.5 \pm 0.6\ \mu m$ was actually 25% larger than the edge-on estimate. The diffraction ring thickness was $0.3 - 0.4\ \mu m$ for both edge-on and face-on measurements, representing uncertainties in absolute values of d and t of $\pm 10\%$ and $\sim \pm 30\%$, respectively.

The shape of platelets seen as flattened discs (face-on) or oblate spheroids (edge-on) is further demonstrated by the micrograph obtained with Nomarski optics (Fig. 3), where the light diffraction effect discussed for phase-contrast microscopy is still inherently present, though no longer visually apparent. Typical $\bar{d}$ and $\bar{t}$ were, respectively, $2.8 \pm 1.1\ \mu m$ ($n = 23$) and $1.4 \pm 0.1\ \mu m$ ($n = 10$), though great uncertainty exists in estimates of t due to the shadow effects (Fig. 3).

The primary geometric parameters ($\bar{d}_{av}, \bar{t}_i$) and those generated by Eqs. 1–4 (rp, V, S, S. I.), as well as associated statistical values, are shown in Table II. The actual histograms are shown in Fig. 4, while data and calculated lines of best fit determined from an analysis of linear regression are shown in Fig. 5 for results where the correlation coefficient r was >0.85. The regression coefficients are shown in Table II for (*i*) r_p vs. each of the other parameters and (*ii*) combinations of the other parameters. All the correlation coefficients shown in Table II had significance $P < 0.05$ or better, except for $r_p - d$, $r_p - S$, $t - S$, and $t - d$ ($P > 0.05$).

Finally, estimates of mean platelet volume, surface area, and sphericity index, and associated statistics, were also made for a disc model with rounded edges, using Eqs. 5–7, as shown in Table III. Similar frequency distributions and correlation coefficients were obtained with this model as for the oblate spheroid model.

Discussion

The purpose of this article is to report data describing the geometry of normal blood platelets in man and in rabbits. Phase contrast studies of normal and hardened

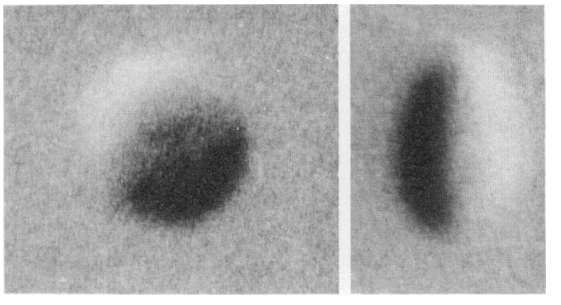

FIGURE 3 View of human, hardened platelets with Nomarski optics instead of phase-contrast. Note shadow effect for edge-on cells (*right*). $\bar{d}$(face-on) $= 3.2 \pm 0.7\ \mu m$ ($n = 20$).

TABLE II

THE GEOMETRIC PARAMETERS AND STATISTICS OF MAMMALIAN PLATELETS: OBLATE SPHEROID MODEL FOR *V*, *S*, S. I. ESTIMATES

		Rabbit platelets directly in plasma; three subjects, sample size $N = 44$				
	Diameter	Thickness	Axis ratio	Volume	Surface area	Sphericity index
	μm	μm		μm^3	μm^2	
Mean $\bar{X}$	3.11	0.59	0.19	3.09	15.78	0.64
SD σ	0.42	0.28	0.09	1.73	4.30	0.17
Skewness G_1	0.11	0.42	0.06	4.45	6.87	0.07
Kurtosis G_2	0.30	0.47	0.00	336	4.35	4.14
Correlation coefficient r*						
(*i*) with r_p	−0.14†	0.96	1.00	0.71	−0.07†	0.99
(*ii*) between	$d - S = 0.99$	$t - V = 0.88$	$V - S = 0.62$	$d - V = 0.56$	$t - S = 0.19$†	$t - d = 0.12$†
		Rabbit platelets, hardened; four subjects, sample size $N = 158$				
Mean $\bar{X}$	3.16	0.62	0.20	3.33	16.48	0.66
SD σ	0.51	0.19	0.07	1.56	5.36	0.14
Skewness G_1	0.15	0.09	0.04	4.88	12.94	0.02
Kurtosis G_2	0.72	0.04	0.00	477	16.00	0.01
Correlation coefficient r*						
(*i*) with r_p	−0.47	0.89	1.00	0.20§	−0.42	0.99
(*ii*) between	$d - S = 0.99$	$t - V = 0.62$	$V - S = 0.75$	$d - V = 0.71$	$t - S = 0.01$†	$t - d = 0.04$†
		Human platelets, hardened; two male subjects, sample size $N = 46$; one 18 yr ($n = 10$) ≡ one 40 yr ($n = 36$)				
Mean $\bar{X}$	3.62	0.93	0.26	7.06	22.15	0.78
SD σ	0.74	0.32	0.08	4.85	9.42	0.15
Skewness G_1	0.52	0.03	0.01	23.42	43.99	0.00
Kurtosis G_2	3.54	0.04	0.00	19.90	148.00	0.00
Correlation coefficient r*						
(*i*) with r_p	−0.14†	0.82	1.00	0.28‖	−0.10†	0.99
(*ii*) between	$d - S = 0.99$	$t - V = 0.76$	$V - S = 0.89$	$d - V = 0.86$	$t - S = 0.46$	$t - d = 0.43$

*Significance $P < 0.0005$, if no indication; §, < 0.01; ‖, < 0.05; †, > 0.05 (from the t test).

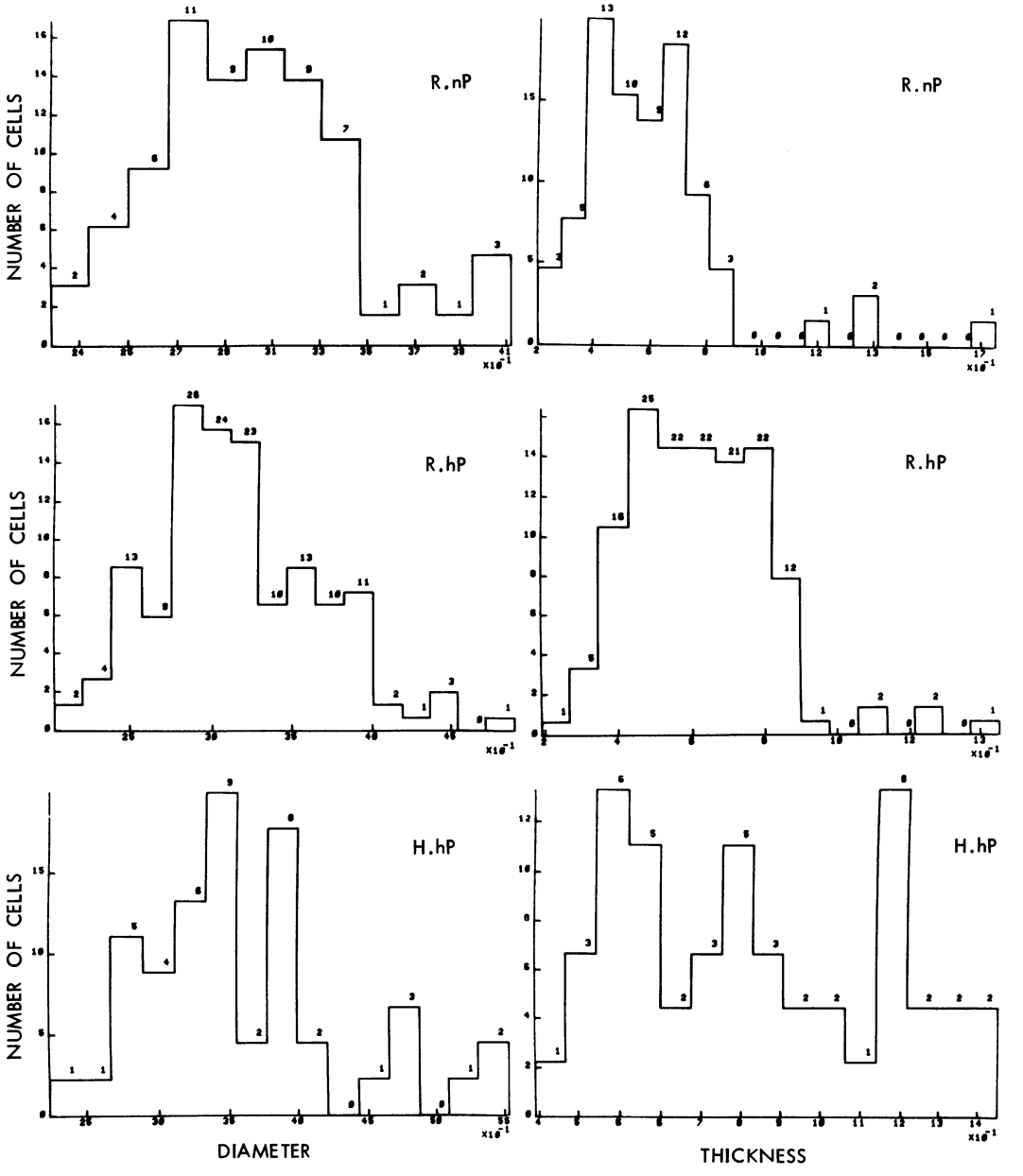

FIGURE 4A Histograms of the first two parameters of Table II. Three rows are shown for diameter and thickness, corresponding to rabbit unfixed platelets in citrated-PRP (R.nP), glutaraldehyde-hardened platelets (R.hP), and hardened human platelets (H.hP).

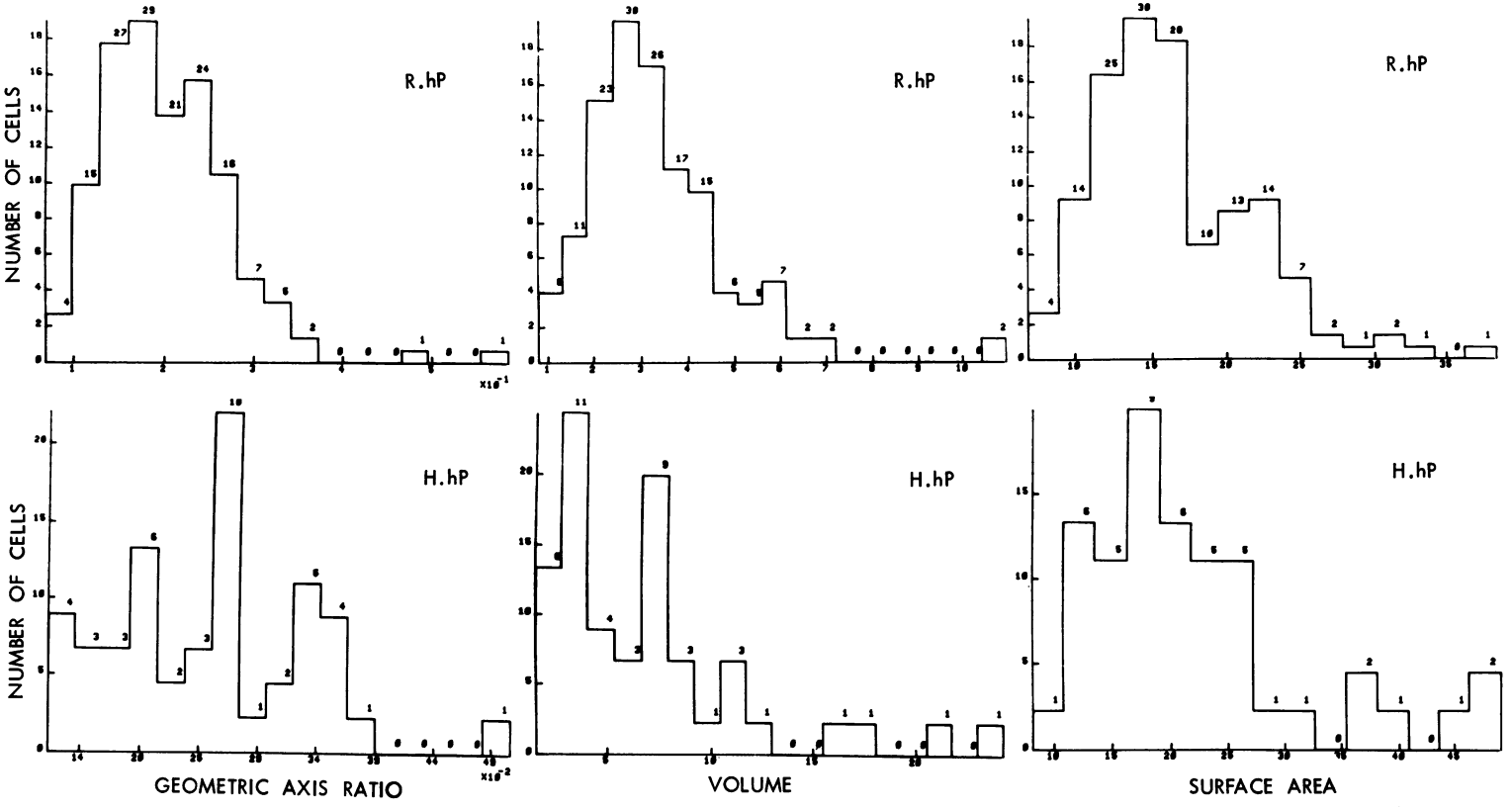

FIGURE 4B Histograms of the last three parameters of Table II. Two rows, for glutaraldehyde-hardened platelets (R.hP) and hardened human platelets (H.hP), are shown.

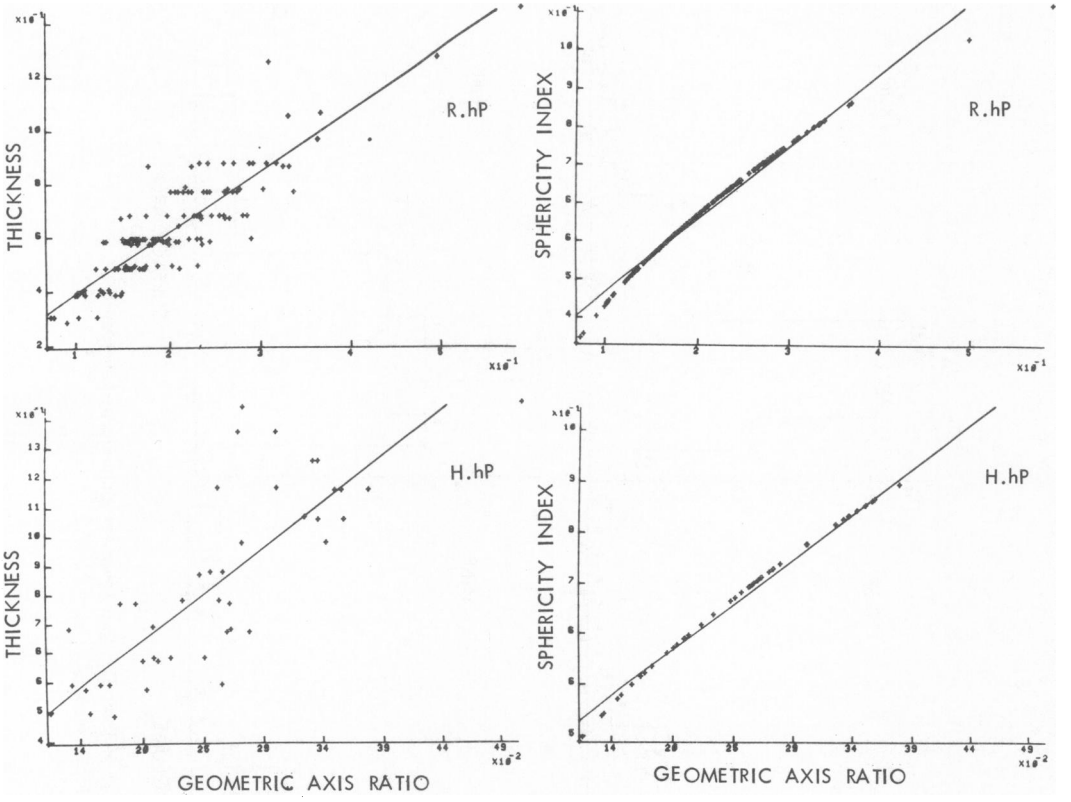

FIGURE 5

erythrocytes, conducted by the empirical technique first introduced by Ponder (1930), as described in the methodology, yielded results for maximum thickness (t_i) and diameters (d_{av}) which compared favorably with the more recent quantitative interference-holographic method (Evans and Fung, 1972), the more difficult estimate of thickness being almost identical in both cases; moreover, geometric axis ratios ($\bar{r}_p$) derived from t and d were identical to values for both rabbit and human erythrocytes obtained by an independent rheo-optical technique (Frojmovic, 1975; Frojmovic et al., 1976). These initial studies gave us confidence in this empirical approach with further support obtained from the comparison of volumes and geometric axis ratios obtained for platelets by independent methods. Fixation conditions were similar to those reported by Shank et al. (1969), who noted no resulting volume change in erythrocytes. Fixation of blood platelets was most important in order to avoid the readily occurring "sphering" artifacts (Barnhart et al., 1972; Frojmovic, 1973; Zucker and Borrelli, 1954).

Diameter and Thickness

Stained human platelets on smears have been analyzed for face-on diameters by Bigel et al. (1967*a*,*b*) using whole blood collected from the peripheral circulation in the

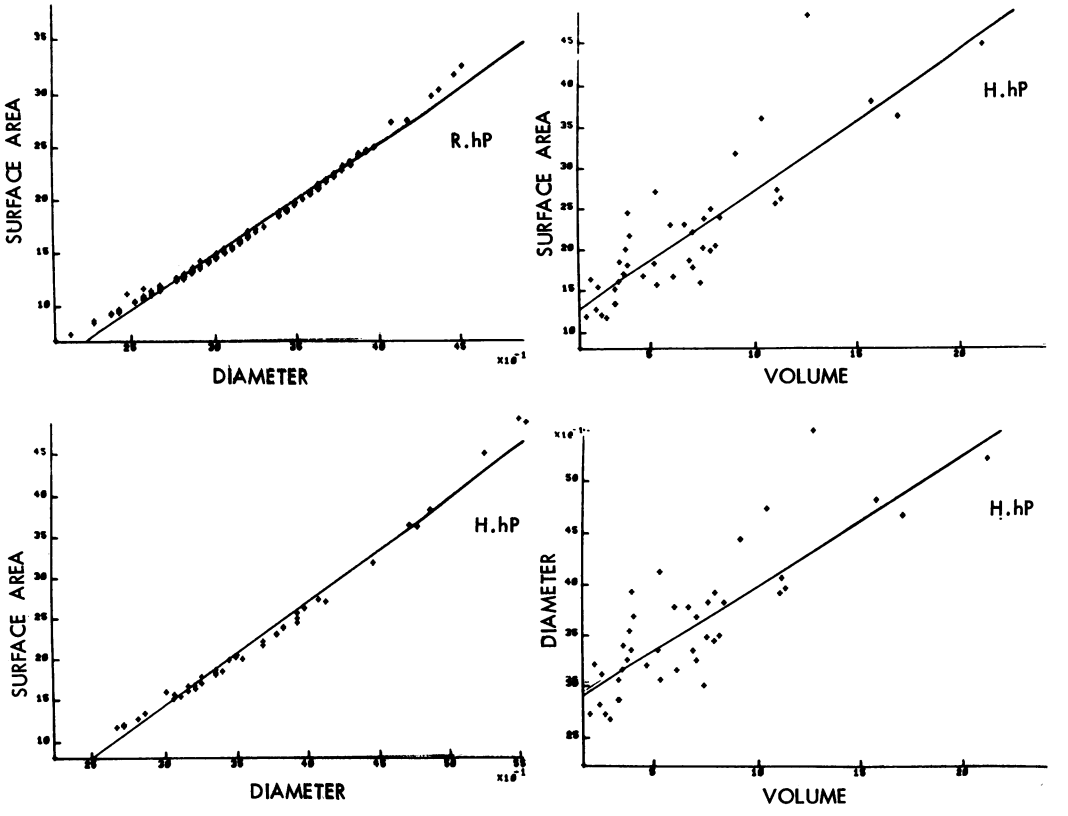

FIGURE 5 Interdependence of some platelet geometric parameters, summarized in Table II ($r > 0.86$). The first three columns show results for hardened human and rabbit platelets while only results for hardened human platelets are shown in the fourth column for $V - S$ (top) and $V - d$ (bottom). Identical curves (not shown) were obtained for normal rabbit platelets.

finger, with reported $\bar{d}$ values (3.1 ± 0.4 μm) only ~15% lower than those reported here, and standard deviation (±13% of mean) about half of that found in our studies, readily accounted for by sphering of some platelets, known to occur at room temperature (Zucker and Borrelli, 1953), which would lead to reduced observable diameters (Frojmovic, unpublished). Given these results, and the identical values for $\bar{d}$, $\bar{t}$, and SD reported for human platelets prepared from fixed whole blood analyzed by transmission electron microscopy (TEM) (Table I), and our own finding that human PRP represents up to about 85% by number of all platelets in blood and appears to be missing a negligible number of large platelets (Table IV), we feel that our results for PRP are probably equally valid for whole blood. This should apply as well to rabbit platelets, for which no reports have appeared to date on $\bar{d}$ and $\bar{t}$ estimates. Comparison of our data with studies of erythrocytes and human platelets with rheo-optical methods (Frojmovic, 1975; Frojmovic et al., 1976) and with other microscopic methods (Fig. 1), suggests that $\bar{d}_{av}$ and $\bar{t}_i$, obtained from edge-on measurements, may represent the proper choices for the geometric $\bar{d}$ and $\bar{t}$ values, respectively. The SD in $\bar{d}$ (±18%) and

TABLE III

PLATELET VOLUMES, SURFACE AREAS, AND SPHERICITY INDICES CALCULATED FOR A "DISC WITH ROUNDED EDGES" MODEL FROM DATA IN TABLE II

	Rabbit platelets in plasma		
	V	S	S. I.
Mean $\bar{X}$	6.49	24.9	0.70
SD σ	4.87	10.7	0.31
Skewness G_1	52	48	0.30
Kurtosis G_2	114,000	259,000	0.22
	Rabbit platelets, hardened		
Mean $\bar{X}$	6.81	26.9	0.74
SD σ	3.42	14.0	0.34
Skewness G_1	16.6	97.6	0.58
Kurtosis G_2	12,100	153×10^4	1.56
	Human platelets, hardened		
Mean $\bar{X}$	15.7	42.6	0.79
SD σ	11.2	29.4	0.30
Skewness G_1	72.4	367	0.13
Kurtosis G_2	481,000	229×10^5	0.13

$\bar{t}$ ($\pm 35\%$) for human and rabbit platelets, respectively, were ~4 times larger than corresponding values for erythrocytes. Data from face-on measurements for $\bar{d}$, using $\bar{d}_{av}$, were consistently larger than those obtained by edge-on measurements for rabbit erythrocytes and human and rabbit platelets, suggesting that $\bar{d}_i$ (Fig. 1) might be a more correct choice of the cell outline in this configuration.

Volume

Platelet sizing has been almost exclusively conducted in terms of volume distributions determined by electronic counters (e.g. Coulter counter), with most studies yielding a

TABLE IV

PLATELET YIELD AND SIZE BIAS FOR PLATELET-RICH PLASMA

Donor type	Yield*		Sample	Percent platelets with diameters†		
	PRP	Platelets in PRP		$\bar{d}$ + ISD	$> 2\bar{d}$	$> 2.3\bar{d}$
	vol %	*no. %*		%	%	%
Human	21–39 (4)§	63–83 (4)	Whole blood	10 (1)	3 (1)	0.25 ± 0.05 (4)
			PRP	20 (1)	1 (1)	0.24 ± 0.09 (4)
Rabbit	32–35 (2)	55–73 (2)	Whole blood	—	0.2–1.4 (3)	0.1–0.5 (3)
			PRP	—	0.2–0.5 (2)	0.1–0.25 (2)

*Analysis as in Materials and Methods; —bias in the samples.

†Only "sphered" platelets were present for whole blood, diluted with ammonium oxalate, so $\bar{d}_s$, calculated for isovolumetric spheres, was 1.9 and 2.2 μm, respectively, for rabbit and human cells.

§These values in brackets indicate the number of different donors studied.

mean volume ($\overline{V}_c$) for "sphered" human platelets from PRP in the range of 7–8 μm^3 (Bull and Zucker, 1965; Enticknap et al., 1969; Karpatkin, 1969), with higher mean values reported for platelets maintained in the "disced" shape upon preparation for counting, both for all platelets present in the blood (7.7 ± 0.2 μm^3; Nakeff and Ingram, 1970) and for platelets from PRP kept at 37°C (8.0 ± 0.2 μm^3; Salzman et al., 1969). A more direct study measuring the packing volume and dead space of human platelets centrifuged in a microhematocrit tube indicated $\overline{V}_p$ = 6.6 μm^3 (Born, 1970). We obtained remarkably similar estimates for $\overline{V}_p$ for human platelets, using our oblate spheroid model (Eq. 3) = 7.1 ± 4.8 μm^3 (see Table II). The standard deviation calculated from our model, yielding a range in $\overline{V}_p$ = 2.3 μm^3 to 11.9 μm^3, is consistent with the reports by Karpatkin (1972) that $\overline{V}_p \simeq 5\ \mu m^3$ for old platelets and $\simeq 12\ \mu m^3$ for young platelets, obtained from packing volume determinations (Karpatkin, 1969). Similarly, the mean platelet volume for rabbit platelets studied with the Coulter counter, $\overline{V}_c$ = 3.2 μm^3 (Herrmann and Griggs, 1967), is in remarkable agreement with our calculated values, consistent with the concept of young and old platelets also reported for animal studies (Maupin, 1970; Hirsh, 1972). Note that estimates of volumes and volume distributions determined for "disced" platelets by the Coulter counter method are subject to considerable uncertainty, due to the effects of shape on the apparent volumes measured, shown both theoretically and experimentally (Grover et al., 1969, 1972; Shank et al., 1969). Our direct measurements are therefore especially important for obtaining volume distributions and associated statistics. Finally, note that for equivalent spheres with the same volume distribution as reported above for human and rabbit platelets, we calculate, using $\overline{V}_s = (\pi/6)\overline{d}_s^3$, greatly reduced mean equivalent sphere diameters, $\overline{d}_s$ = 2.2 μm and 1.9 μm, respectively; i.e., estimates of mean diameter for a population of normal, disced platelets will be low if "sphering" has occurred during preparation and storage, assuming approximately isovolumetric sphering as reported for ADP-sphered human platelets (Born, 1970). This effect might explain the small, mean cross-sectional area reported for formaldehyde-fixed canine platelets by Kraytman (1973) from analyses of face-on orientations in the light microscope. His value of 5.3 ± 0.3 μm^2 corresponds to estimates derived for an equivalent sphere ($[\pi/4]\overline{d}_s^2$ = 4.7 μm^2) with the mean platelet volume being the same as for human platelets, as reported by Nakeff and Ingram (1970). If the shapes of human and canine platelets are similar, the calculated cross-sectional area for the oblate spheroid is 10.5 ± 3.5 μm^2. Thus, either canine platelets are much smaller than human platelets and/or indeed some "sphering" artifacts are present.

Surface Area

Total surface area measurements of blood cells have only been reported for human erythrocytes, with general agreement between the modified Ponder technique (Canham and Burton, 1968; Jay, 1975) and the interference-holographic technique (Tsang, 1974; Evans and Fung, 1972; Evans and Leblond, 1973). Thus, $\overline{S}$ = 129 μm^2, with ±12% SD. Our results for platelets gave $\overline{S}$ = 22.2 μm^2 and 16.5 μm^2, respectively, for human and rabbit platelets, with ~±35% SD. As for $\overline{V}$, larger values (1.5–2 times

greater) were obtained for $\bar{S}$ based on a "disc with rounded edges" model, with SD being much greater ($60 \pm 8\%$) than for the oblate spheroid model.

It is interesting to note that erythrocyte sphering can be accompanied by an isovolumetric change with a decrease in surface area, probably associated with membrane wrinkling, or by an increase in volume with no change in surface area (Jay, 1975), or finally with hemolysis resulting from surface area increases $\geq 20\%$ (Canham and Burton, 1968). For an isovolumetric "sphering" of platelets as reported by Born (1970), we calculate the mean equivalent sphere surface area ($=\pi \bar{d}_s^2$) = 15.2 μm^2 and 11.4 μm^2, respectively for human and rabbit platelets ($\bar{d}_s$ previously indicated). This represents a 31% decrease in surface area from the "disc," which might then account for the associated pseudopodia, i.e. about $\frac{1}{3}$ of the original surface area is converted to pseudopodia. For a sphering associated with conservation of central body surface area, with pseudopodia arising from newly created surface, we calculate $\bar{V}_s$ = 9.5 μm^3 and 6.0 μm^3, corresponding to 31% and 88% increases in volume, respectively, for human and rabbit platelets. Such increases for human platelets have indeed been reported from studies with the uncertain Coulter counter method (Bull and Zucker, 1965; O'Brien, 1970). These models remain to be tested.

Shape Factors

In the case of human platelets, both the mean geometric axis ratio ($\bar{r}_p$ = 0.26) and the sphericity index values ($\overline{S.I.}$ = 0.78 and 0.79 for the "oblate spheroid" and "disc with rounded edges" model, respectively) indicated that these cells have an overall shape identical with that of human or rabbit erythrocytes ($\bar{r}_p$ = 0.29 [Table I]; $\overline{S.I.}$ = 0.78 ± 0.03 [Canham and Burton, 1968]). Rabbit platelets appear much thinner ($\bar{r}_p$ = 0.20; $\overline{S.I.}$ = 0.65) than human platelets or erythrocytes. These same observations were quantitatively confirmed for $\bar{r}_p \pm$ SD by an independent rheo-optical technique (Frojmovic, 1975; Frojmovic et al., 1975; 1976), where an oblate spheroid model was also used for theoretical evaluations. Note that a much lower shape factor ($\overline{S.I.}$ = 0.71) is calculated from $\bar{t}$ and $\bar{d}$ for human platelets considered as simply cylindrical discs (Weast, 1968). Moreover, estimates of $\bar{V}$ (9.7 μm^3) and $\bar{S}$ (31.3 μm^2) were much larger than for the "oblate spheroid" model ($\sim$1.4 times), as observed for $\bar{V}$ and $\bar{S}$ for the "disc with rounded edges" model (1.5–2 times). Finally, the shape of human and rabbit platelets varied much more than that of erythrocytes, as seen from the much larger spread (SD) in r_p (2.5 times) and S. I. (6–10 times).

Frequency Distributions

It is interesting to note that d and t frequency distributions were only slightly skewed with more significant skewness for d for human platelets, in contrast to the highly skewed distributions for calculated volumes and surface areas of mammalian platelets, while both shape factors, r_p and S. I., appeared to have a symmetric frequency distribution about the mean (Table II and Fig. 4). This suggests that the larger platelets may have a wide variation of shapes independent of their size, especially since generally low correlation coefficients were obtained between r_p and volume or surface area

(Table II). This is in contrast to the finding for human erythrocytes where S. I. appeared to decrease with increasing particle volume i.e. older erythrocytes (smaller $\bar{V}$) may be more spherical than younger ones (Canham and Burton, 1968). Kurtosis values for distributions in d, t, r_p, and S. I. indicate flattened distribution curves (except for d for human platelets, where a normal Gaussian distribution is observed), while values for volume and surface area show peaked distributions. These results could be explained by the presence of at least two distinct populations (Hirsh, 1972; Karpatkin, 1972) with varying degrees of overlap of the histograms for these subpopulations for the various geometric parameters. Note that only ~1–3% of all human platelets in our studies had diameters greater than twice the mean diameter (Table IV), similar to a report for platelets observed in stained smears (Bessis, 1973). More detailed analyses await further data.

Correlation Coefficients

As previously reported for similar studies with erythrocytes (Canham and Burton, 1968), a very high positive linear correlation coefficient was found to exist between the geometric axis ratio (r_p), which was found to correlate almost 100% with the sphericity index (S. I.) used as the shape factor to describe erythrocytes, and the mean maximum platelet thickness (t), for both human and rabbit platelets. It thus appears that variations in normal platelet shape are dramatically reflected in platelet thickness. Platelet diameter, on the other hand, correlated almost 100% with total surface area. The correlation coefficient between the axis ratio (r_p) and mean calculated particle volume ($\bar{V}$) or surface area ($\bar{S}$) was generally low, suggesting that large platelets, which may be younger and metabolically and functionally more active (Hirsh, 1972; Karpatkin, 1972; Maupin, 1970), are not necessarily more or less spherical than smaller platelets, as reported for erythrocytes (Canham and Burton, 1968). Finally, a very high positive correlation coefficient was obtained between volume and surface area for human platelets, which, as suggested for erythrocytes (Canham and Burton, 1968), might be explained by the concept of a "minimum cylindrical diameter," representing the thinnest long cylindrical channel through which each cell could theoretically pass, with no increase in area and constant volume. This could lead to a similar model for platelets accounting for a vascular bed "sieving" system for removing cells having some critical geometry. A poorer though highly significant correlation between S-V has been found for rabbit platelets, so that the same argument as above might apply.

CONCLUSIONS

We have presented novel, preliminary data on the geometry of human and rabbit platelets determined by individual particle analysis of freely rotating cells in plasma, with the most appropriate geometric model appearing to be an oblated ellipsoid of revolution. The mean shape factors and volumes correlated excellently with values determined by a number of other methods which could not, however, yield absolute frequency distributions for d, t, and V, and associated parameters. The general sta-

tistical data, derived for cells in platelet-rich plasma, are probably equally valid for whole blood.

These studies of platelet geometry are being extended to include additional normal donors of different ages and sex, studied for fixed samples as well as samples observed directly in plasma at 37°C, including whole blood fixed directly in glutaraldehyde solution. The "disc to sphere" transformation, which normally precedes all of the many platelet functions (adhesion/aggregation, release, clot retraction [Born, 1970]), has not been quantitatively studied to date. The relationship between platelet shape and disease has only been quantitatively reported for May-Hegglin thrombocytopathy using transmission electron microscopy (Lechner et al., 1969), but support for continuing this approach comes from the few known studies of platelet size in disease (Bigel et al., 1967*a,b;* Enticknap et al. 1969; Garg et al., 1971; Kraytman, 1973). Finally, these geometric measurements promise to become clinically practical with the use of image processing systems developed for similar studies of erythrocyte geometry (Eden, 1972; Evans and Leblond, 1973).

The authors are indebted to Prof. M. Levine and Mr. J. Russ (Electrical Engineering Dept.) for Fortran programming and computer print-outs; to Dr. A. Okagawa (Chemistry Dept.) for discussions and derivations of mathematical models; to Doctors R. Birks and B. Baines for the use of their microscopes, respectively, for phase-contrast and Nomarski optics; and to Mr. W. Yung for some technical assistance.

Received for publication 20 January 1976 and in revised form 19 May 1976.

REFERENCES

BARNHART, M. I., R. T. WALSH, and J. A. ROBINSON, 1972. A 3-D view of platelet response to chemical stimuli. *Ann. N.Y. Acad. Sci.* **201**:360.

BESSIS, M. 1973. Living blood cells and their ultrastructure. Springer-Verlag New York, Inc., New York.

BIGEL, P., J. LELLOUCH, S. MAYER, and R. WAITZ. 1967*a*. Le diametre thrombocytaire chez l'adulte normal. *Nouv. Rev. Fr. Hematol.* **7**:900.

BIGEL, P., J. LELLOUCH, S. MAYER, and R. WAITZ. 1967*b*. Les variations pathologique des diametres thrombocytaires. *Nouv. Rev. Fr. Hematol.* **7**:903.

BORN, G. V. R. 1970. Observations on the change in shape of blood platelets. *J. Physiol. (Lond.).* **209**:487.

BULL, B. S., and M. B. ZUCKER. 1965. Changes in platelet volume produced by temperature, metabolic inhibitors, and aggregating agents. *Proc. Soc. Exp. Biol.* **120**:296.

CANHAM, P. B., and A. C. BURTON. 1968. Distribution of size and shape in populations of normal human red blood cells. *Circ. Res.* **22**:405.

CHILD, J. A., W. M. P. BOWRY, and J. P. KNOWLES. 1970. Abnormality of red cell diameter/thickness ratio: findings in iron-deficiency anemia. *Br. J. Haematol.* **19**:251.

EDEN, M. 1972. Image processing techniques in relation to studies of red cell shape. *Nouv. Rev. Fr. Hematol.* **12**:861.

ENTICKNAP, J. B., P. G. GOODING, T. S. LANSLEY, and P. R. D. AVIS. 1969. Platelet size and function in ischaemic heart disease (IHD). *J. Atheroscler. Res.* **10**:41.

EVANS, E. A., and Y. C. FUNG. 1972. Improved measurements of the erythrocyte geometry. *Microvasc. Res.* **4**:335.

EVANS, E. A., and P. F. LEBLOND. 1973. Geometric properties of individual red blood cell discocyte-spherocyte transformations. *Biorheology.* **10**:393.

FROJMOVIC, M. M. 1973. Quantitative parameterization of the light transmission and properties of citrated platelet-rich plasma as a function of platelet and adenosine diphosphate concentrations and temperature. *J. Lab. Clin. Med.* **82**:137.

FROJMOVIC, M. M. 1975. Rheo-optical studies of blood cells. *Bioreheology.* **12**:193.

FROJMOVIC, M. M., and R. PANJWANI. 1975. Blood cell structure-function studies: light transmission and attenuation coefficients of suspensions of blood cell and model particles at rest and with stirring. *J. Lab. Clin. Med.* **86**:326.

FROJMOVIC, M. M., A. OKAGAWA, and S. G. MASON. 1975. Rheo-optical transients in erythrocyte syspensions. *Biochem. Biophys. Res. Commun.* **62**:17.

FROJMOVIC, M. M., M. NEWTON, and H. L. GOLDSMITH. 1976. The microrheology of mammalian platelets: studies of rheo-optical transients and flow in tubes. *Microvasc. Res.* **11**:203.

GARG, S. K., E. L. AMOROSI, and S. KARPATKIN. 1971. Use of the megathrombocyte as an index of megakaryocyte number. *N. Engl. J. Med.* **284**:11.

GOLDSMITH, H. L., and J. MARLOW. 1972. Flow behaviour of erythrocytes. I. Rotation and deformation in dilute suspensions. *Proc. R. Soc. (Lond.).* **B182**:351.

GROVER, N. B., J. NAAMAN, S. BEN-SASSON, and F. DOLJANSKI. 1969. Electrical sizing of particles in suspensions. I. Theory. *Biophys. J.* **9**:1398.

GROVER, N. B., J. NAAMAN, S. BEN-SASSON, and F. DOLJANSKI. 1972. Electrical sizing of particles in suspensions. *Biophys. J.* **12**:1099.

HERRMANN, R. G., and V. G. GRIGGS. 1967. Effect of counting solution and antihistaminics on platelet volume. *Thromb. Diath. Haemorrh.* **18**:705.

HIRSH, J. 1972. Platelet age: its relationship to platelet size, function and metabolism. *Br. J. Haematol.* **23** (Suppl 1):209.

HOVIG, R. 1968. The ultrastructure of blood platelets in normal and abnormal states. *Ser. Hematol.* **1**(2):3.

JAY, A. L. W. 1975. Geometry of the human erythrocyte. I. Effect of albumin on cell geometry. *Biophys. J.* **15**:205.

KARPATKIN, S. 1969. Heterogeneity of human platelets. I. Metabolic and kinetic evidence suggestive of young and old platelets. *J. Clin. Invest.* **48**:1073.

KARPATKIN, S. 1972. Human platelet senescence. *Annu. Rev. Med.* **23**:101.

KRAYTMAN, M. 1973. Platelet size in thrombocytopenias and thrombocytosis of various origin. *Blood.* **41**: 587.

LECHNER, K., K. BREDDIN, K. MOSER, L. STOCKINGER, and E. WENZEL. 1969. May-Hegglinsche Anomalie. *Acta Haematol.* **42**:303.

MAUPIN, B. 1970. Do several populations of platelets exist? *Coagulation.* **3**:119.

NAKEFF, A., and M. INGRAM. 1970. Platelet count: volume relationships in four mammalian species. *J. Appl. Physiol.* **28**:530.

O'BRIEN, J. R. 1970. Platelet function: a guide to platelet membrane structure. *Ser. Haematol.* **111**(4):68.

PONDER, E. 1930. The measurement of the diameter of erythrocytes. V. The relation of the diameter to the thickness. *Q. J. Exp. Physiol.* **20**:29.

RAND, R. P., and A. C. BURTON. 1963. Area and volume changes in hemolysis of single erythrocytes. *J. Cell Comp. Physiol.* **61**:245.

SALTZMAN, E. W., T. P. ASHFORD, D. A. CHAMBERS, L. N. NERI, and A. P. DEMPSTER. 1969. Platelet volume: effect of temperature and agents affecting platelet aggregation. *Am. J. Physiol.* **217**:1330.

SHANK, B. B., R. B. ADAMS, K. D. STEIDLEY, and J. R. MURPHY. 1969. A physical explanation of the bimodel distribution obtained by electronic sizing of erythrocytes. *J. Lab. Clin. Med.* **74**:630.

SHIMAMOTO, T., H. YAMAZAKI, and T. SHIMAMOTO. 1973. Scanning electron microscopic observation of platelets in hemostasis. *Thromb. Diath. Haemorrh.* **29**:168.

TSANG, W. C. O. 1974. The size and shape of human red blood cells. M.Sc. thesis. Dept. of Ames/Bioengineering, University of California, San Diego.

WEAST, R. C. ed. 1968. Handbook of Chemistry and Physics. 43rd edition. The Chemical Rubber Co., Cleveland, Ohio. A-258.

ZUCKER, M. B., and J. BORRELLI. 1954. Reversible alterations in platelet morphology produced by anticoagulants and by cold. *Blood.* **9**:602.